PAPER

Reversible thermochromic fibers with excellent elasticity and hydrophobicity for wearable temperature sensors

Taekyung Lim,[a] Hee Sung Seo,[a] Jonguk Yang,[a] Keun-Hyeok Yang,[b] Sanghyun Ju [iD] *[a] and Sang-Mi Jeong [iD] *[a]

Color-changing fibers, which can intuitively convey information to the human eye, can be used to facilely add functionality to various types of clothing. However, they are often expensive and complex, and can suffer from low durability. Therefore, in this study, we developed highly elastic and hydrophobic thermochromic fibers as wearable temperature sensors using a simple method that does not require an electric current. A thermochromic pigment was embedded inside and outside hydrophobic silica aerogel particles, following which the thermochromic aerogel was fixed to highly elastic spandex fibers using polydimethylsiloxane as a flexible binder. In particular, multi-strand spandex fibers were used instead of single strands, resulting in the thermochromic aerogels penetrating the inside of the strands upon their expansion by solvent swelling. During drying, the thermochromic aerogel adhered more tightly to the fibers by compressing the strands. The thermochromic fiber was purple at room temperature (25 °C), but exhibited a two-stage color change to blue and then white as the temperature increased to 37 °C. In addition, even after 100 cycles of tension-contraction at 200%, the thermochromic aerogel did not detach and was strongly attached to the fiber. Additionally, it was confirmed that color change due to temperature was stable even after exposure to 1 wt% NaCl (artificial sweat) and 0.1 wt% detergent solutions. The developed thermochromic fiber therefore exhibited excellent elasticity and hydrophobicity, and is expected to be widely utilized as an economical wearable temperature sensor as it does not require electrical devices.

1 Introduction

With wearable devices becoming more common, wearable sensor elements that can monitor physiological information (such as blood pressure, heart rate, and body temperature) or environmental information (such as ultraviolet rays, humidity, and temperature) are attracting attention as a core technology.[1-5] In particular, external temperature changes are an important environmental factor that affect the activities of the human body. Exposure to a high-temperature environment for a long time increases the body temperature and disrupts the moisture and salt balance in the body, which can cause heat-related illnesses such as heat stroke, exhaustion, cramps, and fatigue.[6-8] Wearable temperature sensors are a promising technology that have been used in high-temperature environments for several years as a personal healthcare and safety diagnostic system.[9-11] To improve user convenience, wearable temperature sensors are evolving from accessories that are

carried by the user to an integrated form of clothing.[12-15] For sensors to be applied in the form of clothing, in addition to requiring a simple measurement method, external temperature changes must be accurately sensed and effectively displayed, and stable sensing characteristics must be maintained *via* resistance to water and washing.[16-18]

To date, methods to fabricate clothing-integrated or fiber-type wearable temperature sensors include attaching commercially available sensors to existing clothing, attaching conductive fillers to the fabric, and directly converting conductive polymers into fibers by electrospinning.[19-22] The most commercialized temperature sensors detect temperature based on the degree to which resistance increases or decreases with temperature, and do so using conductive materials (such as metallic materials, conductive polymers, nanocarbon materials) that can transmit electrical signals.[23-27] Other methods for detecting temperature include using temperature-sensitive transistors[28,29] or thermoelectric elements that detect temperature differences based on the thermoelectric effect as a voltage;[30,31] these methods have been implemented on stretchable or flexible substrates, and their applicability as wearable temperature sensors has been verified. However, they are cumbersome to install, have complicated structures, require

[a] *Major in Nano Semiconductor, School of Electronic Engineering, Kyonggi University, Suwon, Gyeonggi-do 16227, Republic of Korea. E-mail: shju@kgu.ac.kr*

[b] *Department of Architectural Engineering, Kyonggi University, Suwon, Gyeonggi-do 16227, Republic of Korea. E-mail: jeongsm@kgu.ac.kr*

high production costs owing to high-pressure/high-temperature processing, and are not eco-friendly.[32–34]

Thermochromic sensors utilize materials that reversibly change color at specific temperatures when heated or cooled.[35,36] Several methods have been reported for the fiber of thermochromic materials, including the microencapsulation of thermochromic materials in core-spun yarn for sports clothing or the dying and coating of leather or fabric with thermochromic materials.[37,38] However, spinning of a fiber with a color-changing pigment causes high consumption of the pigment, as well as rapid deterioration of the physical properties of the fiber. Meanwhile, durability is crucial when dyeing or coating microencapsulated fibers in order to prevent dye desorption by washing or friction.[39,40]

In this study, a thermochromic fiber was fabricated as a fiber-type temperature sensor by embedding a hydrophobic thermochromic aerogel inside a highly elastic multi-strand spandex fiber. Thermochromic aerogels were fabricated by coating thermochromic microcapsules onto a silica aerogel, which has a superhydrophobic and porous structure with a high specific surface area. Polydimethylsiloxane (PDMS) was used as a thermal crosslinking binder to stably immobilize the thermochromic material between the spandex strands. The hydrophobic nature of the aerogel prevents contact with water, thereby minimizing the detachment and loss of thermochromic microcapsules and ensuring resistance to sweat and laundry solutions. A reversible color change from purple to blue to white was observed in the temperature range of 25–37 °C, producing an immediate visual effect. The thermochromic color-change reactivity and sensitivity were stably maintained despite the application of external deformation forces such as repeated stretching, environmental exposure using sweat and cleaning solutions, and repeated temperature changes.

2 Experimental

2.1 Fabrication of hydrophobic thermochromic fiber

Hydrophobic thermochromic fibers capable of discoloring at ambient temperature were fabricated by embedding a hydrophobic thermochromic aerogel in spandex fibers (diameter $\sim$ 450 $\pm$ 15 μm; Hyosung TNC Co. Ltd). To synthesize the hydrophobic thermochromic aerogel, 0.4 wt% silica aerogel (diameter $\sim$ 5 μm; JIOS AeroVa®) was added to 50 g of 2-propanol (IPA; 99.5%; DAEJUNG) and ultrasonicated for 5 min. Then, two types of thermochromic pigments purchased from NANO I & C with different color conversion behavior, TP31RE (red at critical temperature 31 °C) and TP35BL (blue at critical temperature 35 °C), were added at 0.55 wt% each, then ultrasonicated for 30 min. In the solution phase, the pigments penetrated the porous structure of the aerogel, resulting in the facile fabrication of hydrophobic thermochromic aerogels; the hydrophobic properties of the aerogel were maintained even after drying. Additionally, to improve the adhesion of the synthesized hydrophobic thermochromic aerogel to fibers, a mixture of the prepolymer PDMS and a curing agent (Sylgard 184, The Dow Chemical Company) at a mass ratio of 10 : 1 was added at a ratio of 0.5 wt% to the solution containing the dispersed

hydrophobic thermochromic aerogel at a concentration of 1.5 wt%; ultrasonication was performed for 30 min to achieve dispersion. Then, the spandex fibers were placed in the hydrophobic thermochromic solution, following which ultrasonication was performed for 30 min to embed the silica aerogel and two types of thermochromic pigments into the spandex fibers. The hydrophobic thermochromic fibers were then removed and dried overnight under room temperature (25 °C). Lastly, a hydrophobic thermochromic textile (20 × 20 mm^2) was fabricated by sewing the hydrophobic thermochromic fibers onto a fabric (21071, ZWEIGART).

2.2 Characterization and analysis of hydrophobic thermochromic fiber

The surfaces and cross-sections of the hydrophobic thermochromic fibers were observed using field-emission scanning electron microscopy (FE-SEM; JSM-7610 PLUS, JEOL). Energy dispersive X-ray spectroscopy (EDS; EDS-7557, Oxford Instruments) was used to determine the elemental distribution of the thermochromic aerogels embedded in the hydrophobic thermochromic fibers. The wettability of the hydrophobic thermochromic fibers was confirmed by measuring the water contact angle using a contact angle analyzer (Phoenix 300, SEO Co). The stress–strain curves of the hydrophobic thermochromic fibers were measured using a thermal mechanical analyzer (TMA; TMA7000, Hitachi). The thermal properties of the hydrophobic thermochromic fiber were measured over a temperature range of 25–800 °C using thermogravimetric analysis (TGA; TGA/DSC1, Mettler Toledo). The hydrophobic thermochromic fibers and textiles were also subjected to a temperature-dependent discoloration test over a temperature range of 25–37 °C using a vacuum oven (SH-VDO-08NG, SH Scientific).

3 Results and discussion

Humans maintain a constant body temperature by regulating the amount of blood near the skin or by expelling sweat through sweat glands. The internal temperature of the human body is 36.8 $\pm$ 0.5 °C, and it is known that the skin temperature needs to be approximately 35 °C to maintain this temperature.[41,42] Despite human body temperature regulation, extreme heat still severely threatens human health and life. It is claimed that there is heat stress to which humans can adapt, expressed as wet-bulb temperature (TW). TW does not exceed 31 °C, and if the external temperature of long-term exposure exceeds 35 °C, hyperthermia may occur because metabolic heat dissipation is impossible.[41,43]

Thermochromic materials have a critical temperature at which they begin to change color in response to temperature stimuli. A series of color-change effects can be obtained by mixing thermochromic dyes at various critical temperatures depending on the end use requirement for recognizing changes in special environments, such as every-day, high-temperature, and military environments. The critical temperature of the hydrophobic thermochromic fiber fabricated in this study was selected to display a color change from room temperature (25 °C) to

a temperature close to the human body temperature (37 °C) for use as a wearable sensor for personal healthcare in everyday environments. In addition, a wearable temperature sensor that can minimize the detachment and loss of thermochromic microcapsules by suppressing their contact with water was fabricated (Fig. 1(a)). The fabricated hydrophobic thermochromic fiber was purple at room temperature (25 °C) and turned white as the temperature increased above 37 °C. Fig. 1(b) shows that when only half of the bundle of thermochromic fibers was immersed in water at 37 °C, the part immersed in water turned white, while the part in the air showed the initial purple color.

Thermochromic materials are materials whose color reversibly changes owing to temperature-dependent changes in their crystalline phases and chemical structures. They are dyes that switch between two chemical structures, one of which is colorless and is called a leuco dye. Leuco dye-based thermochromic materials are generally fabricated using a mixture of leuco-dye, color developer, and solvent contained in the microcapsules, the interactions of which cause color change.[44–46] When the temperature is lower than the melting point of the solvent, the leuco dye and color developer come into contact, and visible color develops through electron interactions. However, when the temperature is higher than the melting point of the solvent, the solvent melts, the leuco dye and color developer separate, and electron interactions do not occur, resulting in a colorless state. In this study, a lactone-based leuco dye was used as the thermochromic material. At low temperatures, it becomes a lactone ring-opening structure and exhibits a visible color, and when the temperature rises, it becomes a lactone ring-closing structure and is colorless.[47–49]

The most common method used to fabricate functional fibers is immersion or dip-coating in a solution in which functional materials are dispersed in the fiber. However, in this case, because the physical interaction between the functional material and fiber surface is weak, there is a possibility that the functional material may leach from the fiber. To prevent this, thermochromic materials were not attached to the fiber as is, but were embedded inside the aerogel, a representative porous structure (Fig. 1(c)). The aerogel used was a silica aerogel with a hydrophobic surface. To fabricate the thermochromic aerogel by embedding thermochromic materials in the internal pores of the porous Si aerogel, ultrasonication was performed by placing the aerogel in an IPA solution in which the thermochromic materials were dispersed. As ultrasonic energy propagates in a solution, it generates a cavitation phenomenon in which fine bubbles are created and destroyed by the pressure of the ultrasonic waves; when these fine bubbles burst, powerful cavitation energy is generated.[50] This energy allowed the thermochromic materials to penetrate not only the surface of the aerogel but also the internal porous structure. Pore structure analysis of pristine and thermochromic aerogels was conducted using N_2 adsorption–desorption isotherms and Brunauer–Emmett–Teller measurements. In both samples, the majority of the uptake occurred in the relative pressure range of 0.95 to 0.10. They exhibited a typical type-IV isotherm, confirming their high-mesoporosity structure. The pristine aerogel has a surface area of 417.46 m^2 g^{-1} and a total pore volume of 1.593 600 cm^3

g^{-1}. Meanwhile, the thermochromic aerogel has a surface area of 1.86 m^2 g^{-1} and a total pore volume of 0.020746 cm^3 g^{-1}. As the thermochromic pigments were impregnated, the porosity of the aerogel decreased, as shown in Fig. 1(d). Subsequently, highly elastic multi-strand spandex fibers were immersed in an IPA solution in which the thermochromic aerogel was dispersed, and ultrasonication was performed. Spandex, a polyether–polyurea copolymer, is not soluble in IPA but swells easily in it,[51] which caused each strand to open. Then, the thermochromic aerogel and PDMS, a binder material in the solution, penetrated the space between the solvent-infiltrated strands via cavitation energy. During the drying process, the opened strands shrank and re-adhered, firmly fixing the infiltrated thermochromic aerogel (Fig. 1(e)).

The fabricated thermochromic aerogel and hydrophobic thermochromic fiber exhibited almost similar purple colors at room temperature (Fig. 1(c) and (f)). In general, the hydrophobic aerogel has very low interaction with spandex, which in turn has strong internal hydrogen bonds with adjacent molecules; however, using this fabrication method, the thermochromic aerogel, which maintains a hydrophobicity of 150°, was easily immobilized on the spandex fiber. In addition, by embedding a thermochromic aerogel, pristine spandex fibers with a water contact angle of 124° were easily fabricated into thermochromic fibers with a hydrophobicity of 145°. Therefore, even when soaked in water, dye desorption was prevented and the color change phenomenon was maintained (Fig. 1(g)). Thermochromic materials coated fiber (without aerogel) and hydrophobic thermochromic fiber (with aerogel) were immersed in 1 wt% NaCl (artificial sweat) and then sonicated for 1 min. When thermochromic materials were coated on spandex fiber without aerogel, the thermochromic materials were slowly leached by dipping the fiber into 1 wt% NaCl (artificial sweat), and the solution turned purple. On the other hand, the hydrophobic thermochromic fiber (with aerogel) did not leach the thermochromic aerogel due to its hydrophobicity; solution remained transparent (Fig. 1(g)).

Fig. 2(a) shows a photograph of the hydrophobic thermochromic fiber, which is purple at room temperature, wound on a transparent threaded bobbin, and Fig. 2(b) shows the FE-SEM and EDS elemental mapping images of the hydrophobic thermochromic fiber. As shown in Fig. 2(b), the hydrophobic thermochromic fiber was fabricated with multiple strands, with a portion of each strand bound together and with a relatively wide space between the strands. The FE-SEM and EDS elemental mapping images showed that the synthesized thermochromic aerogel particles were attached to the surface of each strand. In addition, the presence of the thermochromic aerogel particles was confirmed by tearing off approximately half of the strands that made up the fiber and observing the interior surfaces of the strands. Atomic mapping for Si, which is the main component of the aerogel, showed that the thermochromic aerogel was uniformly coated not only on the outside of the hydrophobic thermochromic fiber but also on the surfaces of the internal strands.

Fig. 2(c) shows the thermal properties of the fiber before and after embedding with the thermochromic aerogel, as obtained from TGA measurements over a temperature range of 25–800 °
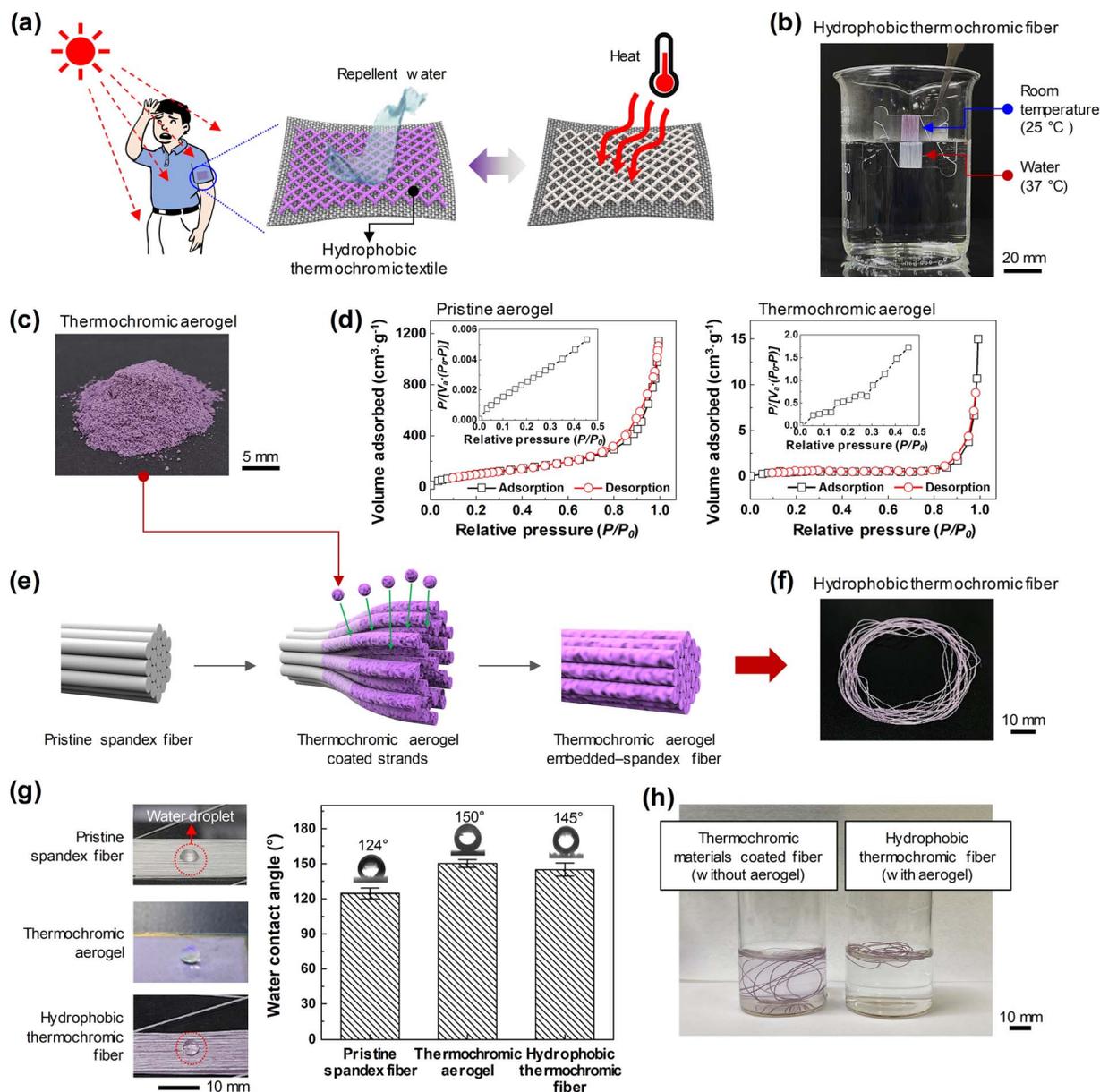
Fig. 1 Reversible thermochromic fibers with hydrophobic and elastic properties. (a) Schematic illustration of the functionality of the hydrophobic thermochromic textile. (b) Photograph of the hydrophobic thermochromic fiber, the color of which changed upon contact with water at 37 °C. (c) Photograph of the thermochromic aerogel. (d) Nitrogen adsorption–desorption isotherms and Brunauer–Emmett–Teller curve of pristine aerogel and thermochromic aerogel. (e) Schematic diagram of the hydrophobic thermochromic fiber fabrication process. (f) Photograph of the hydrophobic thermochromic fiber with embedded thermochromic aerogel. (g) Water contact angles of the pristine spandex fiber, thermochromic aerogel, and hydrophobic thermochromic fiber. (h) Image of the thermochromic materials coated fiber and hydrophobic thermochromic fiber immersed in 1 wt% NaCl (artificial sweat).

C. The thermal decomposition of the fibers was accomplished in two stages. At 250 °C, a weight loss was observed owing to the decomposition of thermally unstable urethane groups (hard segments). Then, at 450 °C, weight loss occurred owing to the decomposition of the soft segment, polyol.[52] The weight loss of the fibers continued until ~650 °C, above which all the polymer chains decomposed, resulting in the mass converging to almost 0%. Comparing the weight loss curves of the pristine and hydrophobic thermochromic fibers, the initial thermal stability of the hydrophobic thermochromic fiber was slightly lower than

that of the pristine spandex fiber. This is presumed to be because of a reduction in weight caused by the decomposition of the heat-vulnerable organic materials (thermochromic materials, Si–CH$_3$ groups on the aerogel, and PDMS binder) used to fabricate the hydrophobic thermochromic fiber. The TGA data show that the expansion/contraction process undergone by the spandex fiber for embedding the thermochromic aerogel did not have a significant effect on the thermal properties of the fiber.
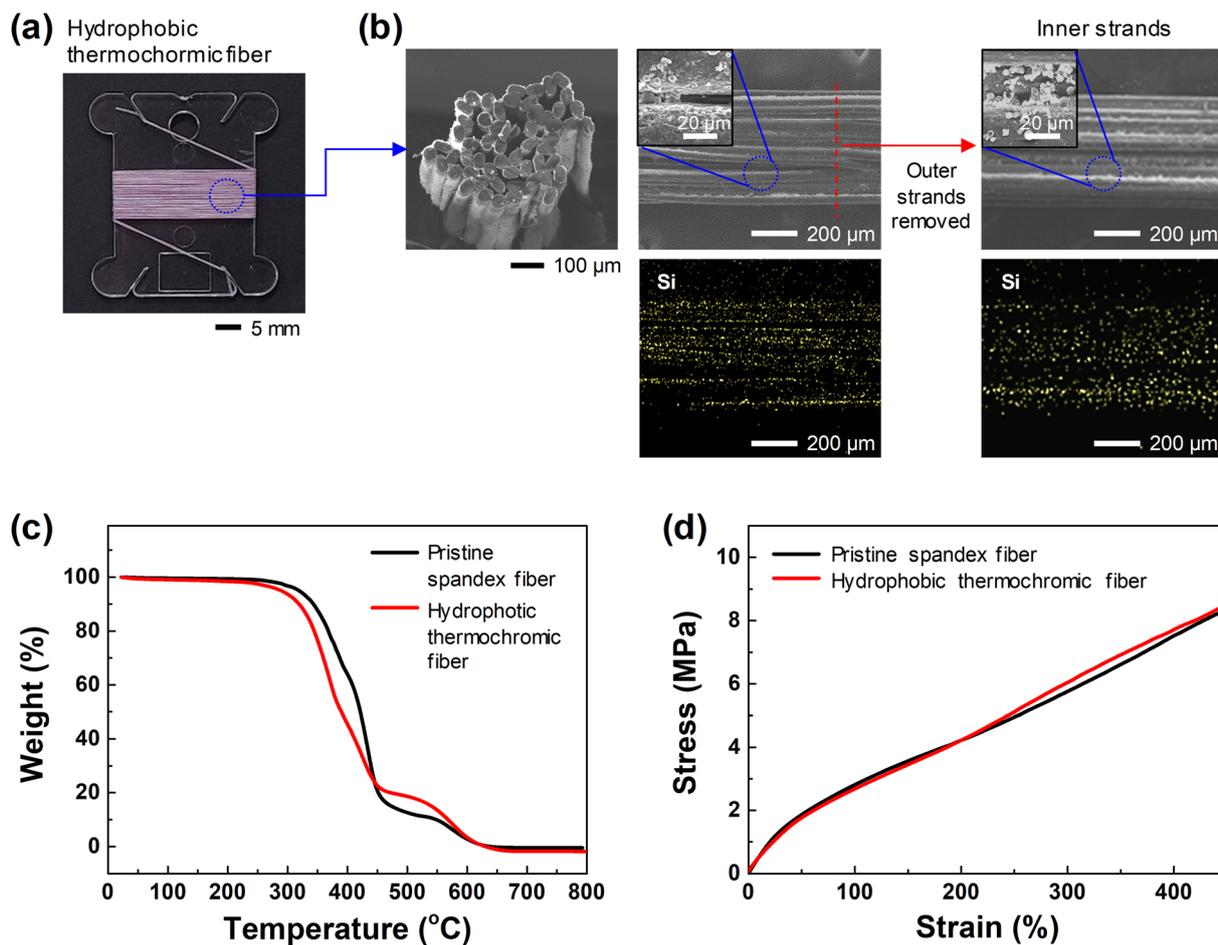
Fig. 2 Characterization of hydrophobic thermochromic fiber. (a) Photograph of hydrophobic thermochromic fiber. (b) FE-SEM and EDS elemental mapping images of thermochromic aerogels embedded in the outer and inner strands of the hydrophobic thermochromic fiber. (c) TGA thermograms and (d) stress–strain curves of the pristine spandex fiber and hydrophobic thermochromic fiber.

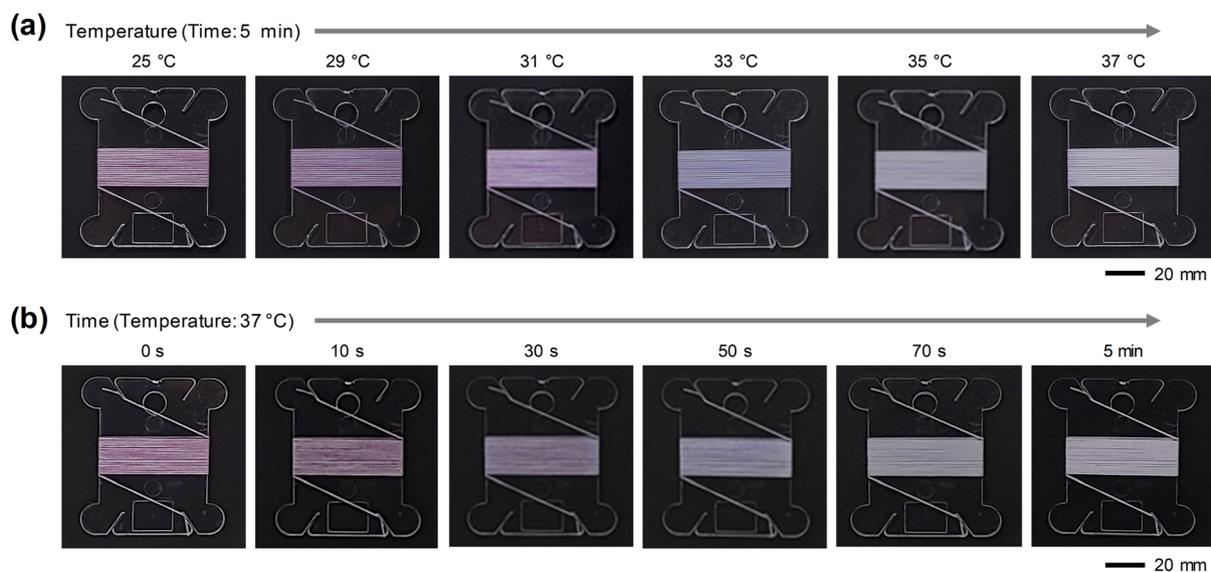Fig. 3 Real-time colorimetric response of hydrophobic thermochromic fiber. (a) Photographs depicting the color change of the hydrophobic thermochromic fiber in the temperature range of 25–37 °C when maintained for 5 min. (b) Photographs of continuous color change of hydrophobic thermochromic fiber for 0–5 min at a temperature of 37 °C.
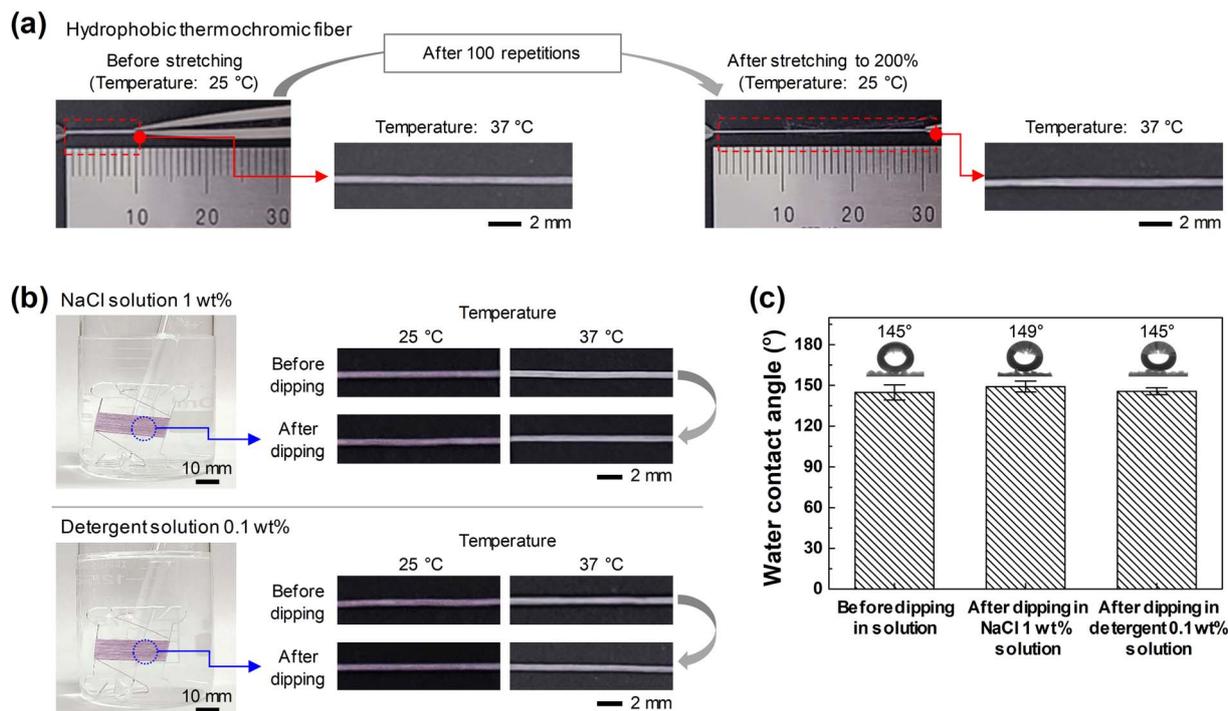
Fig. 4 Chemical and physical durability of hydrophobic thermochromic fiber. (a) Stability in color change of the hydrophobic thermochromic fiber upon 100 stretching-restoration cycles at more than 200%. Comparison of (b) color change and (c) hydrophobicity characteristics before and after exposure of thermochromic fiber to 1 wt% NaCl solution and 0.1 wt% detergent solution.

Wearable sensors that can be attached to clothing must exhibit excellent mechanical properties, including elasticity and flexibility, to maintain their performance during various human body movements. The hydrophobic thermochromic fiber fabricated in this study comprised a highly elastic spandex composed of multiple stands as the matrix; therefore, upon stretching, its elasticity was almost restored. As shown in Fig. 2(d), even when the initial 1 mm hydrophobic thermochromic fiber was stretched to 5 mm (400%), the maximum length allowed by the TMA, the fiber did not break. The coating method developed in this study can therefore express the characteristics of the embedded functional material while maintaining the high elasticity of the spandex.

Fig. 3 shows the real-time color change that occurred when the fabricated hydrophobic thermochromic fiber was wrapped around a transparent threaded bobbin and heated at room temperature. As shown in Fig. 3(a), the color change of the hydrophobic thermochromic fiber was confirmed by sequentially increasing the temperature from room temperature (25 °C) to 37 °C with a temperature-holding time of 5 min. The hydrophobic thermochromic fiber, which was initially purple at 25 °C, changed to blue at ~33 °C, and finally white, the original color of spandex fiber, when heated to above 37 °C. To check the reaction rate of color change, the temperature was maintained at 37 °C, and the color change was observed over time. As shown in Fig. 3(b), the color changed immediately when the temperature was increased, becoming light purple after ~30 s, blue at ~50 s, and white when the temperature was maintained for ~5 min. The hydrophobic thermochromic fiber returned to its

initial purple color within approximately 5 min at room temperature. Therefore, it was confirmed that the hydrophobic thermochromic fiber could intuitively and reversibly sense and respond to changes in the external temperature.

Coating functional materials on fibers is economical because it consumes less energy than the mixed spinning method used with polymers; however, there is a risk of the functional materials detaching from the fibers. In particular, when using staple fibers, additives such as binders are essential to increase the adhesion between the functional material and the fiber; however, this is not a perfect solution for preventing the desorption of the functional material. Meanwhile, when a yarn-type fiber is used, as in this study, the functional material can be fixed to the fiber using a relatively economical coating method such as ultrasonication, and the possibility of detachment can be further reduced by using a small amount of binder. In this study, to ensure the convenience of application to wearable sensors, the use of highly elastic spandex fibers was proposed to maintain colorimetric sensing characteristics even when stretched at 200%. To enable its application in clothing, a process was added to verify durability of the colorimetric functionality even through sweat, rain, and washing.

First, to confirm the durability of the fiber against mechanical deformation, the initial 1 mm thermochromic fiber was subjected to 100 tension-contraction cycles at 200% or more, then exposed to a temperature of 37 °C, and the color change observed (Fig. 4(a)). The color change was found to be the same as that of the initial sample, confirming that the thermochromic aerogel embedded in the hydrophobic thermochromic fiber

(a) Hydrophobic thermochromic textile

Temperature
25 °C   33 °C   37 °C

10 mm

(b)   Temperature: 25 °C

33 °C

37 °C
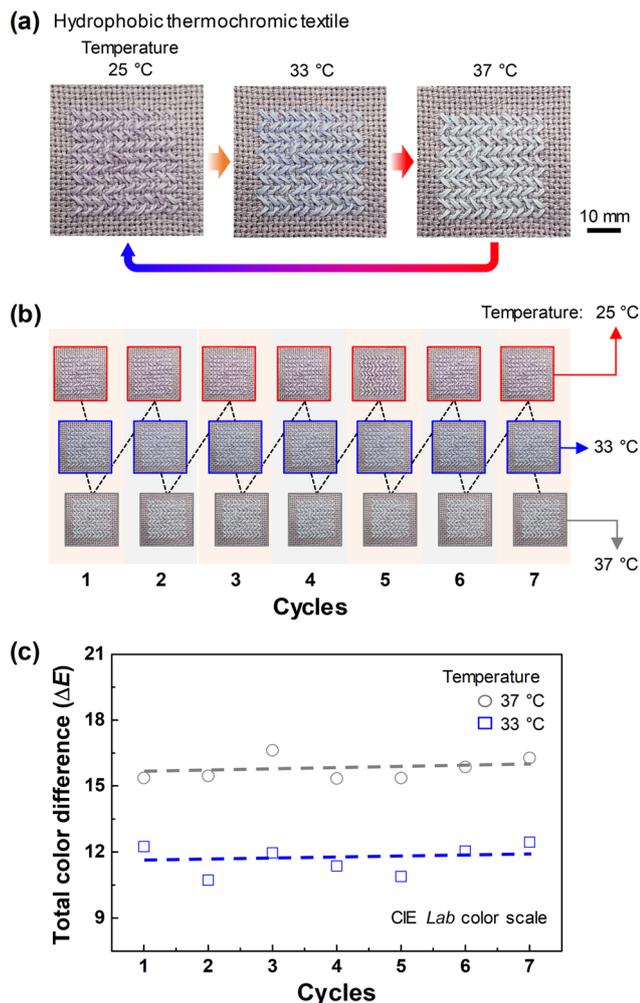
1   2   3   4   5   6   7
Cycles

Fig. 5 Reliability of hydrophobic thermochromic textile against temperature changes. (a) Schematic of color change of hydrophobic thermochromic textile at 25, 33, and 37 °C. (b) Photographs depicting color change and (c) plot of total color difference (ΔE) of hydrophobic thermochromic textile with changes in temperature (25, 33, and 37 °C) for seven cycles.

was stably distributed, even after the fiber was stretched and contracted. In addition, to confirm its stability when exposed to rain, sweat, and washing, the hydrophobic thermochromic fiber was dipped into a 1 wt% NaCl solution and 0.1% detergent solution for 10 min each while wound around the threaded bobbin. A 1 wt% NaCl solution was prepared as the artificial sweat solution because, while sweat is mostly water, it is an aqueous solution containing a small amount (0.2–1 wt%) of solute, the largest proportion of which is NaCl.[53] Meanwhile, to simulate the effect of washing, a conventional laundry detergent (Power Soda Bubble Bright, Mukunghwa, South Korea), which can be easily purchased, was dissolved in water. As shown in Fig. 4(b), the color change in response to temperature changes was stable even after the hydrophobic thermochromic fiber was exposed to the solutions. In addition, it was confirmed that the fiber maintained almost similar hydrophobic properties (Fig. 4(c)). This proves that the hydrophobic thermochromic

fiber fabricated using our coating method exhibits high physical and chemical durability as a wearable sensor, even under conditions such as wrinkling (contraction), stretching, sweating, and washing.

For application as a wearable sensor for personal healthcare in everyday environments, hydrophobic thermochromic textiles were fabricated by sewing the hydrophobic thermochromic fibers into cross-stitch fabrics (Fig. 5(a)). When the fabricated hydrophobic thermochromic textile was exposed to temperatures of 25, 33, and 37 °C, the color of the hydrophobic thermochromic textile changed to purple, blue, and white, respectively. To confirm the reversibility of the color change, the same textile was repeatedly heated and cooled at temperatures of 25, 33, and 37 °C for 10 min each, repeated seven times, and it was observed whether the color change characteristics remained constant. As shown in Fig. 5(b), the color at each temperature remained constant even though the heating (temperature-on) and cooling (temperature-off) cycles were repeated seven times. Because each person can perceive colors differently, the International Commission of Illumination (CIE) $L^*a^*b^*$ color space analysis method was used to analyze the color changes as objective values. The CIE $L^*a^*b^*$ color space analysis method is an identification method that evaluates the color difference between a standard sample and the sample to be measured. Therefore, in order to make the color change of the hydrophobic thermochromic fiber more apparent, a purple fabric with a similar color to that of the hydrophobic thermochromic fiber at room temperature was selected for comparison. The samples of both fabrics were photographed at the same location and lighting conditions, and the images were analyzed using ADOBE PHOTOSHOP CS4 to extract the CIE $L^*a^*b^*$ color-space values of the samples. ΔE was then calculated from the extracted color-space values using the following equation:

$$\Delta E = [(\Delta L^*)^2 + (\Delta a^*)^2 + (\Delta b^*)^2]^{1/2}$$

where $\Delta L^* = L - L_0$; $\Delta a^* = a - a_0$; $\Delta b^* = b - b_0$. L_0, a_0, b_0 are the measured values for the hydrophobic thermochromic fiber (standard sample) at room temperature (25 °C).[54] The ΔE value for the temperature on–off cycles was 11.7 ± 0.7 at 33 °C and 15.8 ± 0.5 at 37 °C, and remained almost constant for each cycle (Fig. 5(c)). Thus, it was confirmed that the color change remained constant even upon repeated exposure to each temperature.

4 Conclusions

In this study, hydrophobic thermochromic aerogels embedded with thermochromic materials were synthesized and coated onto highly elastic multi-strand spandex fibers. The resulting hydrophobic thermochromic fibers underwent minimal loss of thermochromic materials from exposure to water, sweat, or laundry solutions owing to the porous structure and hydrophobic properties of the aerogel. In addition, during the expansion/contraction of the spandex fibers during fabrication, detachment was prevented by the aerogel particles fixing

themselves between the multiple strands of the spandex fiber. The fabricated hydrophobic thermochromic fiber is intended for use as a wearable sensor for personal healthcare in every-day environments. It showed a two-stage reversible color change from room temperature (25 °C) to a temperature close to the human body temperature (37 °C), initially changing from purple to blue and then to white, the natural color of the spandex fiber. In addition, even after performing 100 tension-contraction cycles at 200%, the thermochromic aerogel did not desorb, confirming the reliability of the color change. The fiber also exhibited hydrophobic properties with a water contact angle of 145°, owing to which its color change behavior was stable even after exposure to water, sweat, and laundry solutions. The hydrophobic thermochromic fibers developed in this study can be easily sewn into a variety of products, including clothing and accessories. It is lightweight, durable, and does not require electricity. Therefore, it is expected to be widely utilized as a wearable temperature sensor.

Conflicts of interest

The authors declare no completing financial interests.

Acknowledgements

References

1 S. Qian, M. Liu, Y. Dou, Y. Fink and W. Yan, *Natl. Sci. Rev.*, 2023, **10**(1), nwac202.

2 J. V. Vaghasiya, C. C. Mayorga-Martinez and M. Pumera, *npj Flexible Electron.*, 2023, **7**, 26.

3 Y. Zhang, H. Wang, H. Lu, S. Li and Y. Zhang, *iScience*, 2021, **24**(7), 102716.

4 Z. Deng, L. Guo, X. Chen and W. Wu, *Sensors*, 2023, **23**, 2479.

5 Y. Su, C. Ma, J. Chen, H. Wu, W. Luo, Y. Peng, Z. Luo, L. Li, Y. Tan, O. M. Omisore, Z. Zhu, L. Wang and H. Li, *Nanoscale Res. Lett.*, 2020, **15**, 200.

6 J. Wu, Z. Wu, Y. Wei, H. Ding, W. Huang, X. Gui, W. Shi, Y. Shen, K. Tao and X. Xie, *ACS Appl. Mater. Interfaces*, 2020, **12**, 19069–19079.

7 V. Trovato, S. Sfameni, G. Rando, G. Rosace, S. Libertino, A. Ferri and M. R. Plutino, *Molecules*, 2022, **27**, 5709.

8 T. W. Son, D. A. Ramli and A. A. Aziz, *Procedia Comput. Sci.*, 2021, **192**, 3686–3695.

9 V. Patel, A. Chesmore, C. M. Legner and S. Pandey, *Adv. Intell. Syst.*, 2022, **4**, 2100099.

10 S. Shakerian, M. Habibnezhad, A. Ojha, G. Lee, Y. Liu, H. Jebelli and S. Lee, *Saf. Sci.*, 2021, **142**, 105395.

11 A. Saidi and C. Gauvin, *J. Therm. Biol.*, 2023, **113**, 103405.

12 M. Gao, P. Wang, L. Jiang, B. Wang, Y. Yao, S. Liu, D. Chu, W. Cheng and Y. Lu, *Energy Environ. Sci.*, 2021, **14**, 2114–2157.

13 Y. Peng, J. Dong, J. Sun, Y. Mao, Y. Zhang, J. Long, L. Li, C. Zhang, Y. Zhao, H. Lu, H.-L. Qian, X.-P. Yan, J. Zhao, F. Wang, Y. Huang and T. Liu, *Nano Energy*, 2023, **110**, 108374.

14 P. Lugoda, J. C. Costa, C. Oliveira, L. A. Garcia-Garcia, S. D. Wickramasinghe, A. Pouryazdan, D. Roggen, T. Dias and N. Münzenrieder, *Sensors*, 2020, **20**, 73.

15 A. Tsolis, S. Bakogianni, C. Angelaki and A. A. Alexandridis, *Sensors*, 2023, **23**, 3289.

16 J. Luo, S. Gao, H. Luo, L. Wang, X. Huang, Z. Guo, X. Lai, L. Lin, R. K. Y. Li and J. Gao, *Chem. Eng. J.*, 2021, **406**, 126898.

17 M. Lou, I. Abdalla, M. Zhu, X. Wei, J. Yu, Z. Li and B. Ding, *ACS Appl. Mater. Interfaces*, 2020, **12**, 19965–19973.

18 B. Arman Kuzubasoglu and S. Kursun Bahadir, *Sens. Actuators, A*, 2020, **315**, 112282.

19 J. Shi, S. Liu, L. Zhang, B. Yang, L. Shu, Y. Yang, M. Ren, Y. Wang, J. Chen, W. Chen, Y. Chai and X. Tao, *Adv. Mater.*, 2020, **32**, 1901958.

20 J. Cai, M. Du and Z. Li, *Adv. Mater. Technol.*, 2022, **7**, 2101182.

21 A. Nag, R. B. V. B. Simorangkir, D. R. Gawade, S. Nuthalapati, J. L. Buckley, B. O'Flynn, M. E. Altinsoy and S. C. Mukhopadhyay, *Mater. Des.*, 2022, **221**, 110971.

22 R. R. Ruckdashel, N. Khadse and J. H. Park, *Sensors*, 2022, **22**, 6055.

23 R. Fu, X. Zhao, X. Zhang and Z. Su, *Chem. Eng. J.*, 2023, **454**, 140467.

24 Y. Yu, S. Peng, P. Blanloeuil, S. Wu and C. H. Wang, *ACS Appl. Mater. Interfaces*, 2020, **12**, 36578–36588.

25 R. Nishimoto, Y. Sato, J. Wu, T. Saizaki, M. Kubo, M. Wang, H. Abe, I. Richard, T. Yoshinobu, F. Sorin and Y. Guo, *Biosensors*, 2022, **12**, 559.

26 M. Krifa, *Textiles*, 2021, **1**, 239–257.

27 A. F. Al Naim and A. G. El-Shamy, *Mater. Sci. Semicond. Process.*, 2022, **152**, 107041.

28 S. Rahmani Charvadeh and J. Ghalibafan, *Biosens. Bioelectron.: X*, 2022, **12**, 100264.

29 C. Harito, L. Utari, B. R. Putra, B. Yuliarto, S. Purwanto, S. Z. J. Zaidi, D. V. Bavykin, F. Marken and F. C. Walsh, *J. Electrochem. Soc.*, 2020, **167**, 037566.

30 Y. Wang, Z. Zhou, J. Zhou, L. Shao, Y. Wang and Y. Deng, *Adv. Energy Mater.*, 2022, **12**, 2102835.

31 Y. Zheng, H. Liu, X. Chen, Y. Qiu and K. Zhang, *Org. Electron.*, 2022, **106**, 106535.

32 W. Root, T. Bechtold and T. Pham, *Materials*, 2020, **13**, 626.

33 H. Ullah, M. A. Wahab, G. Will, M. R. Karim, T. Pan, M. Gao, D. Lai, Y. Lin and M. H. Miraz, *Biosensors*, 2022, **12**, 630.

34 Y. Liu, S. Shang, S. Mo, P. Wang and H. Wang, *Int. J. Precis. Eng. Manuf. - Green Technol.*, 2021, **8**, 1323–1346.

35 Z. Zhang, Y. Liu, K. Yang, D. Chen, S. Li and Z. Li, *Mater. Chem. Phys.*, 2022, **290**, 126564.

36 H. Ramlow, K. L. Andrade and A. P. S. Immich, *J. Text. Inst.*, 2021, **112**, 152–171.

37 X. Liu, J. Miao, Q. Fan, W. Zhang, X. Zuo, M. Tian, S. Zhu, X. Zhang and L. Qu, *Adv. Fiber Mater.*, 2022, **4**, 361–389.

38 J. Chen, H. Wen, G. Zhang, F. Lei, Q. Feng, Y. Liu, X. Cao and H. Dong, *ACS Appl. Mater. Interfaces*, 2020, **12**, 7565–7574.

39 A. S. Farooq and P. Zhang, *Composites, Part A*, 2021, **142**, 106249.

40 L. Civan and S. Kurama, *Mater. Sci. Technol.*, 2021, **37**, 1405–1420.

41 S. C. Sherwood and M. Huber, *Proc. Natl. Acad. Sci. U. S. A.*, 2010, **107**, 9552–9555.

42 E. G. Hanna and P. W. Tait, *Int. J. Environ. Res. Public Health*, 2015, **12**, 8034–8074.

43 C. Raymond, T. Matthews and R. M. Horton, *Sci. Adv.*, 2020, **6**, eaaw1838.

44 O. Panák, M. Držková and M. Kaplanová, *Dyes Pigm.*, 2015, **120**, 279–287.

45 A. Hakami, S. S. Srinivasan, P. K. Biswas, A. Krishnegowda, S. L. Wallen and E. K. Stefanakos, *J. Coat. Technol. Res.*, 2022, **19**, 377–402.

46 A. N. Bourque and M. A. White, *Can. J. Chem.*, 2015, **93**, 22–31.

47 G. Kim, S. Cho, K. Chang, W. S. Kim, H. Kang, S.-P. Ryu, J. Myoung, J. Park, C. Park and W. Shim, *Adv. Mater.*, 2017, **29**, 1606120.

48 S. Cho, G. Kim, S. Lee, J. Park and W. Shim, *Adv. Opt. Mater.*, 2017, **5**, 1700627.

49 W. Oh, S. Angupillai, P. Muthukumar, H.-S. So and Y. Son, *Dyes Pigm.*, 2016, **128**, 235–245.

50 I. Tudela, Y. Zhang, M. Pal, I. Kerr and A. J. Cobley, *Surf. Coat. Technol.*, 2014, **259**, 363–373.

51 Y. Cui, H. Wang, H. Pan, T. Yan and C. Zong, *J. Appl. Polym. Sci.*, 2021, **138**, 51346.

52 R. F. Magnago, N. D. Müller, M. Martins, H. R. T. Silva, P. Egert and L. Silva, *Polímeros*, 2017, **27**, 141–150.

53 S. J. Montain, S. N. Cheuvront and H. C. Lukaski, *Int. J. Sport Nutr. Exerc. Metab.*, 2007, **17**, 574–582.

54 X. Yan, Y. Chang and X. Qian, *Polymers*, 2020, **12**, 552.